Quantum statistical physics of glasses at low temperatures

J. van Baardewijk and R. Kühn
Department of Mathematics, King's College University–London, Strand, London WC2R 2LS, United Kingdom
(Received 22 September 2009; revised manuscript received 21 December 2009; published 2 February 2010)

We present a quantum statistical analysis of a microscopic mean-field model of structural glasses at low temperatures. The model can be thought of as arising from a random Born von Karman expansion of the full interaction potential. The problem is reduced to a single-site theory formulated in terms of an imaginary-time path integral using replicas to deal with the disorder. We study the physical properties of the system in thermodynamic equilibrium and develop both perturbative and nonperturbative methods to solve the model. The perturbation theory is formulated as a loop expansion in terms of two-particle irreducible diagrams, and is carried to three-loop order in the effective action. The nonperturbative description is investigated in two ways, (i) using a static approximation and (ii) via quantum Monte Carlo simulations. Results for the Matsubara correlations at two-loop order perturbation theory are in good agreement with those of the quantum Monte Carlo simulations. Characteristic low-temperature anomalies of the specific heat are reproduced, both in the nonperturbative static approximation, and from a three-loop perturbative evaluation of the free energy. In the latter case the result so far relies on using Matsubara correlations at two-loop order in the three-loop expressions for the free energy, as self-consistent Matsubara correlations at three-loop order are still unavailable. We propose to justify this by the good agreement of two-loop Matsubara correlations with those obtained nonperturbatively via quantum Monte Carlo simulations.

DOI: 10.1103/PhysRevB.81.054203 PACS number(s): 63.50.Lm

I. INTRODUCTION

Glasses are known to exhibit distinctive low-temperature properties that differ substantially from those of crystalline solids and are referred to as glassy low-temperature anomalies. For instance, at low temperatures the specific heat and thermal conductivity in crystals show a familiar T^3 dependence. In glasses the specific heat is found to increase approximately linearly with the temperature at $T<1$ K while the thermal conductivity increases approximately as T^2 in this low-temperature range.[1] At higher temperatures between 1 and 20 K the thermal conductivity is approximately constant while the specific heat C shows a peak when displayed as C/T^3, usually referred to as the Bose peak. In phenomenological models such as the standard tunneling model[2,3] and the soft-potential model[4,5] one postulates that a broad spectrum of tunneling centers is responsible for the properties at $T<1$ K.

Surprisingly, the glassy anomalies show a noticeable degree of universality at $T<1$ K whereas between approximately 1 and 20 K these depend more on the specific materials.[1] There are currently two main contending theories to explain this fact. Following ideas of Yu and Leggett,[6] it has been suggested as resulting from a collective effect due to interactions between the tunneling excitations.[7] Alternatively, it is thought to be a property of the potential-energy landscape created by glassy freezing at high temperatures. This also defines a phenomenon of collective origin but involves no quantum effects.[8] Universality in the second interpretation is understood as a result of separation of the energy scales involved in glassy freezing on the one hand side and those relevant for the low-temperature phenomena on the other hand side.[8,9] Whereas the existence of tunneling centers is part of the initial assumptions in Ref. 7, these are shown to arise naturally as a result of *microscopic* interactions in the model glasses studied in Refs. 8 and 9 and do indeed give rise to the characteristic low-temperature anomalies. The work in Refs. 8 and 9 is perhaps appropriately characterized as a strong-coupling approach to glassy low-temperature physics. A complementary weak-coupling approach[10,11] to the same phenomena takes weak residual interactions between a set of quasilocal collective modes as starting point and describes low-temperature anomalies in terms of a vibrational instability occurring in systems of this type.

The analysis in Refs. 8 and 9 is still semiclassical in the sense that it is based on an analysis of quantum effects in a glassy potential-energy landscape whose properties were determined via classical statistical mechanics. The aim of the present paper is to overcome this deficit and study the system in a full quantum statistical formulation right from the outset. Focus will be here on the translationally invariant model proposed in Ref. 9.

We shall proceed along the lines of general methods developed for quantum spin glasses. In particular, we apply the Matsubara formalism to construct an imaginary-time path-integral representation of the partition function and the replica method to deal with the disorder. The sites are decoupled by introducing order parameters for which the functional integral is evaluated by the method of steepest descent. The result is an effective single-site theory and a set of functional self-consistency relations for the order parameters. These methods are similar to those used for models studying spin-glass transitions in quantum spin glasses. Examples are the SK model of spin glasses generalized to quantum spins[12] and the quantum spherical p-spin-glass model.[13,14] Here we shall not concern ourselves with the glass transition but concentrate on evaluating the physical properties at low temperatures and, in particular, the specific-heat anomaly in the 1 K region.

To solve the effective single-site theory we first apply a perturbative method in terms of two-particle irreducible

(2PI) diagrams, which is based on an expansion in powers of the full-interacting correlation functions. This amounts to summing infinite classes of diagrams and can therefore also capture effects of a nonperturbative nature. After this we develop a nonperturbative theory proper. The result is a set of functional self-consistency equations for the order parameters which we first treat with quantum Monte Carlo (QMC) simulations.

Following this we construct a *solvable* version of the nonperturbative theory, using a simple approximation known from quantum spin-glass theory as the *static* approximation. This scheme was first introduced as a variational Ansatz in Ref. 12 where the time-dependent order parameter was approximated by a time-independent constant.

Given the complications of dealing with quantum fluctuations in this model, we presently restrict the analysis of both perturbative and nonperturbative theories to the replica-symmetric approximation. In support of this we mention that the effects of replica symmetry breaking (RSB) on the low-temperature anomalies were found to be small at the semiclassical level.[8,9]

This paper is organized as follows. In Sec. II we summarize the main ingredients of the proposed glass model. In Sec. III we give the many-particle partition function represented by an imaginary-time path integral and introduce replicas to handle the disorder averaging. Section IV gives an account of the effective single-site formulation, deriving the effective action and the functional self-consistency relations for the order parameters. Then in Sec. V we treat perturbative and in Sec. VI nonperturbative solution methods. The numerical results for the order parameters and the specific heat are discussed in Sec. VII. Finally, the conclusions are drawn in Sec. VIII.

II. GLASS MODEL

Starting point is the microscopic model for a glasslike system at low temperatures, proposed in Ref. 9. To summarize its main ingredients, consider a system of N degrees of freedom (called particles) with the following model Hamiltonian:

$$H = T + V = \sum_{i=1}^{N} \frac{p_i^2}{2m_i} + V(\boldsymbol{u}), \tag{1}$$

where the p_i denote the momenta and the m_i the masses, which for simplicity are taken equal for each particle. The variables $\boldsymbol{u}=(u_1,\ldots,u_N)$ represent coordinate deviations from preassigned reference positions. Since glassy low-temperature physics is universal, the interaction potential $V(\boldsymbol{u})$ need not contain details of the specific atoms and their specific interactions and is taken as simple as possible, yet containing enough detail to reproduce glassy low-temperature physics. The minimum requirement is that it should respect global translation invariance and have elements of randomness and frustration. There are two possibilities to make analytic progress: use a mean-field approximation for a microscopically "semirealistic" model or alternatively formulate a model for which such a mean-field approximation would be exact. The latter is the approach we have taken here, a justification of which we believe is provided by the results. The absence of phonons is of course one of the unavoidable consequences of adopting a mean-field approximation.

Following Ref. 9, the potential function is taken to represent the first terms of a Born von Karman expansion of the full interaction energy about the reference positions. A further requirement of global Z_2 symmetry ($\boldsymbol{u}\leftrightarrow-\boldsymbol{u}$) excludes the odd orders in this expansion. Matters are further simplified by taking the u_i to be scalar, resulting in

$$V(\boldsymbol{u}) = \sum_{i<j}^{N} \left[\frac{1}{2} J_{ij}(u_i - u_j)^2 + \frac{g}{N}(u_i - u_j)^4 \right]. \tag{2}$$

The glassy properties are represented at the quadratic level in Eq. (2), defining a random-interaction term with random-interaction strengths J_{ij}. The quartic term (taken to be non-random) is necessary in order to stabilize the system as a whole and so $g>0$. The parameters J_{ij} are quenched and taken independent with equal Gaussian distribution $\mathcal{N}(0,J^2/N)$ for each combination (i,j). The $1/N$ scaling of the variance and the quartic interaction term in Eq. (2) ensures that the thermodynamic energy is proportional to N. The construction as presented here allows the system to be analyzed within replica mean-field theory, similar to that of the SK model for spin glasses,[15] its generelisation to quantum spin glasses,[12] and quantum spherical p-spin glasses.[13,14]

III. PARTITION FUNCTION

The quantum statistical partition function for the fixed disorder configuration $\{J_{ij}\}$ in a basis of coordinate states $|\boldsymbol{u}\rangle=|u_1\rangle\ldots|u_N\rangle$ is

$$Z_J = \mathrm{Tr}\,\exp(-\beta\hat{H}) = \int d\boldsymbol{u}\langle\boldsymbol{u}|\exp(-\beta\hat{H})|\boldsymbol{u}\rangle, \tag{3}$$

where the Hamiltonian $\hat{H}$ is defined by Eq. (1) with u_i and p_i replaced by the operators $\hat{u}_i$ and $\hat{p}_i$. In the Matsubara formalism the path-integral representation of Eq. (3) is constructed using the Lie-Trotter product formula[16,17]

$$\exp(-\beta\hat{T}-\beta\hat{V}) = \lim_{r\to\infty}\left\{\exp\left(-\frac{\beta\hat{T}}{r}\right)\exp\left(-\frac{\beta\hat{V}}{r}\right)\right\}^r. \tag{4}$$

Insertions of $\hat{1}=\int d\boldsymbol{u}_k|\boldsymbol{u}_k\rangle\langle\boldsymbol{u}_k|$ and $\hat{1}=\int d\boldsymbol{p}_k|\boldsymbol{p}_k\rangle\langle\boldsymbol{p}_k|$, together with definitions of imaginary time $\tau_k=k\Delta\tau$ $(k=0,\ldots,r-1)$ and time step $\Delta\tau=\frac{\hbar\beta}{r}$, leads to the following path-integral representation of Eq. (3):

$$Z_J = \int \mathcal{D}\boldsymbol{u}\,\exp\left(-\frac{1}{\hbar}\mathcal{A}[\boldsymbol{u}]\right), \tag{5}$$

where the integration is in the functional sense with a measure defined as

$$\mathcal{D}\boldsymbol{u} = \lim_{r\to\infty} \prod_{k=0}^{r-1} \prod_{i=1}^{N} \sqrt{\frac{mr}{2\pi\hbar^2\beta}} du_i(\tau_k). \tag{6}$$

The functions $u_i(\tau)$ satisfy the periodicity conditions $u_i(0) = u_i(\hbar\beta)$. The Euclidean action reads

$$\mathcal{A}[\boldsymbol{u}] = \int_0^{\hbar\beta} d\tau \left\{ \sum_{i=1}^{N} \frac{m}{2} \left(\frac{du_i(\tau)}{d\tau} \right)^2 + V[\boldsymbol{u}(\tau)] \right\}. \tag{7}$$

The interaction potential $V[\boldsymbol{u}(\tau)]$ equals the expression in Eq. (2) with u_i replaced by $u_i(\tau)$.

In order to study the equilibrium properties of the model we need to compute the disorder averaged free-energy density f. The replica trick[18] allows us to evaluate this as

$$-\beta f = \frac{1}{N}\overline{\log Z_J} = \lim_{n\to 0} \frac{1}{Nn} \log \overline{(Z_J)^n}, \tag{8}$$

where the overline denotes the average over all realizations of the random interaction. To end this section we list the expression for $(Z_J)^n$, i.e., the replicated version of Eq. (5),

$$(Z_J)^n = \int \prod_{a=1}^{n} \mathcal{D}\boldsymbol{u}^a \exp\left(-\frac{1}{\hbar} \sum_{a=1}^{n} \mathcal{A}[\boldsymbol{u}^a] \right). \tag{9}$$

The index a numbers the replicas and $\boldsymbol{u}^a = (u_1^a, \ldots, u_N^a)$.

IV. EFFECTIVE SINGLE-SITE FORMULATION

In order to evaluate Eq. (8) we first average over all realizations of the random potential. This is achieved by carrying out the independent Gaussian integrations over the set $\{J_{ij}\}$. The result is

$$\overline{(Z_J)^n} = \int \prod_{a=1}^{n} \mathcal{D}\boldsymbol{u}^a \exp\left[\sum_{i<j} \left\{ \frac{J^2}{8\hbar^2 N} \left(\sum_a \int d\tau [u_i^a(\tau) - u_j^a(\tau)]^2 \right)^2 - \frac{g}{\hbar N} \sum_a \int d\tau [u_i^a(\tau) - u_j^a(\tau)]^4 \right\} \right]$$
$$\times \exp\left[-\frac{1}{\hbar} \sum_{ia} \int d\tau \frac{m}{2} \dot{u}_i^a(\tau)^2 \right]. \tag{10}$$

The expansions of the powers in the first line of Eq. (10) contain many terms that vanish due to the following Ansatz. We assume the global Z_2 symmetry to remain unbroken after quantization, $1/N\Sigma_i u_i^a(\tau) = 0$ for all $\tau \in [0, \hbar\beta]$. This means that we do not have to consider terms of the kind $\Sigma_{ij}\Sigma_{ab}\int d\tau \int d\tau' u_i^a(\tau)^2 u_i^b(\tau') u_j^b(\tau')$, which would complicate the formulation considerably. The result after the expansions is

$$\overline{(Z_J)^n} = \int \prod_{ia} \mathcal{D}u_i^a \exp\left(\sum_{ab} \int d\tau d\tau' \left\{ \frac{J^2}{4\hbar^2 N} \left[\sum_i u_i^a(\tau) u_i^b(\tau') \right]^2 + \frac{J^2}{8\hbar^2} \sum_i u_i^a(\tau)^2 u_i^b(\tau')^2 \right\} \right.$$
$$\left. - \frac{1}{\hbar} \sum_a \int d\tau \left\{ \sum_i \left[\frac{m}{2} \dot{u}_i^a(\tau)^2 + g u_i^a(\tau)^4 \right] + \frac{3g}{N} \left[\sum_i u_i^a(\tau)^2 \right]^2 \right\} \right). \tag{11}$$

The sites are decoupled with two sets of Gaussian transformations after which Eq. (11) becomes

$$\overline{(Z_J)^n} = \int \mathcal{D}\{q_{aa}(\tau,\tau)\} \mathcal{D}\{q_{ab}(\tau,\tau')\}$$
$$\times \exp\left\{ N \left(-\frac{1}{\hbar} \mathcal{X}[q] + \log Z_{\text{eff}} \right) \right\}, \tag{12}$$

where Z_{eff} defines the effective single-site partition function

$$Z_{\text{eff}} = \int \prod_a \mathcal{D}u_a \exp\left(-\frac{1}{\hbar} \mathcal{S}_{\text{eff}}[u_a] \right). \tag{13}$$

The nonfluctuating part in Eq. (12) is defined as

$$\mathcal{X}[q] = \frac{J^2}{4\hbar} \sum_{ab} \int d\tau d\tau' q_{ab}(\tau,\tau')^2 - 3g \sum_a \int d\tau q_{aa}(\tau,\tau)^2. \tag{14}$$

The effective single-site action reads

$$\mathcal{S}_{\text{eff}}[u_a] = \frac{1}{2} \sum_{ab} \int d\tau d\tau' u_a(\tau) q_{0,ab}^{-1}(\tau,\tau') u_b(\tau') + \mathcal{S}_{\text{int}}[u_a]. \tag{15}$$

The interaction part $\mathcal{S}_{\text{int}}[u_a]$ contains a quartic term nonlocal in time and quartic term local in time,

$$\mathcal{S}_{\text{int}}[u_a] = -\frac{J^2}{8\hbar} \sum_{ab} \int d\tau d\tau' u_a(\tau)^2 u_b(\tau')^2 + g \sum_a \int d\tau u_a(\tau)^4. \tag{16}$$

The "free" inverse propagator is

$$q^{-1}_{0,ab}(\tau,\tau') = \left\{ -m\frac{d^2}{d\tau^2} + 12g q_{aa}(\tau,\tau) \right\} \delta_{ab}\delta(\tau-\tau') - \frac{J^2}{\hbar} q_{ab}(\tau,\tau'). \tag{17}$$

Observe here that $\mathcal{S}_{\text{eff}}[u_a]$ in Eq. (13) and thus also Z_{eff}, depend functionally on $q_{ab}(\tau,\tau')$.

The replicated partition function [Eq. (12)] can be treated with the saddle-point method. At the saddle points we have

$$\overline{(Z_J)^n} \sim \exp\left\{ N\left(-\frac{1}{\hbar}\mathcal{X}[q] + \log Z_{\text{eff}} \right) \right\}, \tag{18}$$

where the saddle-point fields $q_{ab}(\tau,\tau')$ are the order parameters of the theory. The saddle-point equations result in the following functional self-consistency relations for the order parameters:

$$q_{ab}(\tau,\tau') = \langle u_a(\tau) u_b(\tau') \rangle. \tag{19}$$

The angular brackets $\langle \cdots \rangle$ denote the quantum thermodynamical average mediated by the effective action [Eq. (15)]. The order parameters $q_{ab}(\tau,\tau')$ are the full-interacting correlation functions of the single-site theory, from here on called Matsubara correlations.

The Matsubara correlations are time-translational invariant since we are studying an equilibrium problem. They are also symmetric in time due to the time-reversal invariance of the action [Eq. (15)], i.e., we have

$$q_{ab}(\tau,\tau') = q_{ab}(\tau-\tau') = q_{ab}(\tau'-\tau). \tag{20}$$

Furthermore the Matsubara correlations $q_{ab}(\tau-\tau')$ are $\hbar\beta$ time periodic.

We should mention that the first interaction term in Eq. (16) defines a complete square, which could be linearized at the cost of introducing a Gaussian family of systems. However, we have chosen not to do this at this stage. It would lead to more complicated saddle-point equations for the order parameters when solving the single-site theory perturbatively. However, we shall linearize this interaction term in the nonperturbative treatment.

V. PERTURBATION THEORY

A. 2PI-effective action formalism

To solve the single-site theory perturbatively, we need a formalism that expands the path integral [Eq. (13)] in terms of a further effective (classical) action $\Gamma_{\text{eff}}[q]$,

$$Z_{\text{eff}}[q] = \int \prod_a \mathcal{D}u_a \exp\left(-\frac{1}{\hbar}\mathcal{S}_{\text{eff}}[u_a,q] \right) = \exp\left(-\frac{1}{\hbar}\Gamma_{\text{eff}}[q] \right). \tag{21}$$

Here we have explicitly referred to the functional dependences on the Matsubara correlations in $\mathcal{S}_{\text{eff}}[u_a,q]$ and in $Z_{\text{eff}}[q]$. Remember, this dependence is due to the appearance of $q_{ab}(\tau,\tau')$ in the inverse propagator [Eq. (17)]. The $q_{ab}(\tau,\tau')$ define the *full-interacting* correlations as we saw in the previous section. As regards to a perturbative expansion of the path integral, the most efficient way is to also express $\Gamma_{\text{eff}}[q]$ entirely in terms of the full-interacting correlations, which was already assumed in the notation in Eq. (21). For this we choose the 2PI-effective action approach, developed in field theory,[19,20] which is indeed based on an expansion of $\Gamma_{\text{eff}}[q]$ in powers of the full-interacting correlators $q_{ab}(\tau,\tau')$ and involves only 2PI diagrams. The 2PI nature of the diagrams has the additional advantage of considerably reducing the number of diagrams that need to be included in the expansion. Also, as the expansion is in terms of the full-interacting correlators, the 2PI approach effectively amounts to summing infinite classes of diagrams of a conventional perturbation expansion, thus enabling it to capture effects of a nonperturbative nature. Usefulness of the 2PI-effective action approach for the study of stochastic dynamical systems was advocated in Ref. 21. Its application to the analysis of glassy systems was suggested in Ref. 22.

Before presenting the series expansion of $\Gamma_{\text{eff}}[q]$, we discuss the key ingredients of the 2PI-effective action approach, in a formulation appropriate for the present problem. Following Ref. 19, one first adds a two-body source term to the action $\mathcal{S}_{\text{eff}}$. This defines a generating functional

$$Z_{\text{eff}}[K,q] = \int \prod_a \mathcal{D}u_a \exp\left(-\frac{1}{\hbar}\left\{ \mathcal{S}_{\text{eff}}[u_a,q] + \frac{1}{2}\sum_{ab}\int d\tau d\tau' u_a(\tau) K_{ab}(\tau,\tau') u_b(\tau') \right\} \right) \equiv \exp\left(-\frac{1}{\hbar} W_{\text{eff}}[K,q] \right), \tag{22}$$

giving

$$\frac{\delta W_{\text{eff}}[K,q]}{\delta K_{ab}(\tau,\tau')} = \frac{1}{2} q_{ab}(\tau,\tau'). \tag{23}$$

From Eqs. (14) and (22) follows

$$\frac{\delta W_{\text{eff}}[K,q]}{\delta q_{ab}(\tau,\tau')} + \frac{1}{\hbar}\frac{\delta \mathcal{X}[q]}{\delta q_{ab}(\tau,\tau')} = 0. \tag{24}$$

We shall need this in the equations of motion for $q_{ab}(\tau,\tau')$, to be constructed next. In order to eliminate K in favor of the full-interacting correlations q, one performs the following Legendre transformation:

$$\Gamma_{\text{eff}}[q] = W_{\text{eff}}[K,q] - \frac{1}{2}\sum_{ab}\int d\tau d\tau' q_{ab}(\tau,\tau') K_{ab}(\tau,\tau'), \tag{25}$$

giving

$$\frac{\delta \Gamma_{\text{eff}}[q]}{\delta q_{ab}(\tau,\tau')} = \frac{\delta W_{\text{eff}}[K,q]}{\delta q_{ab}(\tau,\tau')} - \frac{1}{2} K_{ab}(\tau,\tau'). \tag{26}$$

Then setting the source field $K_{ab}(\tau,\tau')$ to zero and using Eq. (24) results in the following "equations of motion" for $q_{ab}(\tau,\tau')$,

$$\frac{\delta \Gamma_{\text{eff}}[q]}{\delta q_{ab}(\tau,\tau')} + \frac{1}{\hbar}\frac{\delta \mathcal{X}[q]}{\delta q_{ab}(\tau,\tau')} = 0. \tag{27}$$

Next is to describe the series expansion of $\Gamma_{\text{eff}}[q]$, which we present in the standard form as derived in Refs. 19 and 20,

$$\Gamma_{\text{eff}}[G] = \frac{\hbar}{2}\text{Tr}\, q_0^{-1}G + \frac{\hbar}{2}\text{Tr}\log G^{-1} + \sum_{p=2}^{\infty}\Gamma_p[G] \quad (28)$$

with Green's function $G_{ab}(\tau,\tau') \equiv q_{ab}(\tau,\tau')/\hbar$. As already mentioned, the variable $q_{ab}(\tau,\tau')$ defines the full-interacting correlation functions and satisfies the equations of motion [Eq. (27)]. The traces are taken in the functional sense. The first two terms in Eq. (28) define what is called the one-loop contribution. The terms denoted by $\Gamma_p[G]$ define the p-loop contributions. These are represented by 2PI diagrams containing p loops. In the next section we shall discuss the rules for constructing such diagrams. A diagram is said to be 2PI if it does not become disconnected upon cutting two lines. The fact that the contributions $\Sigma_{p=2}^{\infty}\Gamma_p[G]$ define 2PI diagrams is understood from the following argument. The equations of motion [Eq. (27)] with substitutions of Eqs. (14) and (28) just result in the Dyson equations,

$$G^{-1} = q_0^{-1} + 2\frac{\delta}{\delta G}\left(\sum_{p=2}^{\infty}\Gamma_p[G] + \frac{1}{\hbar}\mathcal{X}[G]\right). \quad (29)$$

Since the second part of Eq. (29) defines the proper self-energy, the diagrams of which are known to be one-particle irreducible, clearly the diagrams of the terms $\Gamma_p[G]$ must be 2PI, (the diagrams of $\mathcal{X}[G]$ are 2PI). In the expansion of 2PI diagrams we shall consider two orders, the two-loop order and the three-loop order. They are analyzed in Secs. V C and V D below.

One should mention that Eq. (28) is only valid for the special case $\langle u_a(\tau)\rangle = 0$. If $\langle u_a(\tau)\rangle \equiv \mathcal{U}_a \neq 0$ a further source term in Eq. (22) is needed. This would lead to extra terms depending on $\mathcal{U}_a$ in the effective action [Eq. (28)], and a further equation of motion $\delta\Gamma_{\text{eff}}/\delta\mathcal{U}_a = 0$.[19] We shall not concern ourselves with this case since we have assumed global symmetry to remain unbroken, i.e., $\langle u_a(\tau)\rangle = 0$ (see Sec. IV).

In the 2PI-effective action formalism the classical form (21) results in the following expression for free energy:

$$\beta f^{(\text{2PI})} = \lim_{n\to 0}\frac{1}{n\hbar}(\mathcal{X}[q] + \Gamma_{\text{eff}}[q]), \quad (30)$$

where we have used Eqs. (8) and (18).

B. Rules for 2PI diagrams

The two interaction terms in Eq. (16) determine the following rules for constructing 2PI diagrams and their expressions. Vertices are labeled by a replica index and a time variable. Two vertices labeled by (a,τ) and (b,τ') are connected by a solid line contributing a factor $\hbar G_{ab}(\tau,\tau') = q_{ab}(\tau,\tau')$. The two interaction terms define two types of vertices. First, there is a g-type vertex which is represented by a dot • and contributes a factor $-g/\hbar$. Second, there is a J-type vertex which is represented by a cross $\times$. The J-type vertices always come in sets of two. The two are connected by a dashed line $\times---\times$. A dashed line contributes a factor $J^2/8\hbar^2$. Each diagram gets an extra factor $-\hbar$ due to the prefactor $-1/\hbar$ in Eq. (13). Then there is a further permutational factor to consider which we write in front of the diagram. Next is to collect all factors of a diagram and multiply them. Finally, one needs to sum over all replica indices and integrate over all time variables.

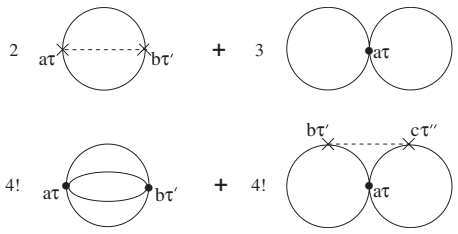

FIG. 1. Two-loop and three-loop 2PI diagrams.

When constructing diagrams of order p, all distinct diagrams containing p loops are added together, resulting in the final expression for $\Gamma_p[q]$. When counting loops, both solid lines and dashed lines need to be considered. The number of loops in a diagram is equal to the power of $\hbar$ in its expression. A subtlety here is that when counting powers of $\hbar$, one factor $\hbar$ in the contribution of each dashed line $J^2/8\hbar^2$ must not be taken into account. This is the factor $\hbar$ that originates from the coupling constant $J^2/8\hbar$ of the nonlocal interaction term in Eq. (16), which represents an interaction parameter as a whole. Finally, it should be noted that each expansion order $\Gamma_p[q]$ contains diagrams of $\mathcal{O}(n)$ in replica and diagrams of $\mathcal{O}(n^2)$ or higher order. Since $n\to 0$ the latter can be ignored.

The 2PI diagrams for two-loop order $(p=2)$ and three-loop order $(p=3)$ are given in Fig. 1. The prefactors here result from permutations.

C. Two-loop order

The two-loop 2PI diagrams are shown in the first line of Fig. 1. According to the rules listed in Sec. V B these diagrams represent the following expressions:

$$\Gamma_2[q] = -\frac{J^2}{4\hbar}\sum_{ab}\int d\tau d\tau' q_{ab}(\tau,\tau')^2 + 3g\sum_a\int d\tau q_{aa}(\tau,\tau)^2, \quad (31)$$

where we have used $q_{ab}(\tau,\tau') = \hbar G_{ab}(\tau,\tau')$. The equations for the two-loop Matsubara correlations $q_{ab}(\tau,\tau')$ are derived from the equations of motion [Eq. (27)], resulting in

$$0 = \frac{1}{2}q_{0,ab}^{-1}(\tau,\tau') - \frac{\hbar}{2}q_{ab}^{-1}(\tau,\tau') - \frac{J^2}{2\hbar}q_{ab}(\tau,\tau') + 6g\delta_{ab}\delta(\tau-\tau')q_{aa}(\tau,\tau). \quad (32)$$

These were solved in a replica symmetric approximation and using Fourier transform techniques as described in Sec. VII B 1 below.

D. Three-loop order

The three-loop 2PI diagrams are shown in the second line of Fig. 1. These diagrams represent the following expressions:

$$\Gamma_3[q] = -\frac{12g^2}{\hbar}\sum_{ab}\int d\tau d\tau' q_{ab}(\tau,\tau')^4 + \frac{3J^2g}{\hbar^2}\sum_{abc}\int d\tau d\tau' d\tau'' q_{ab}(\tau,\tau')^2 q_{ac}(\tau,\tau'')^2. \tag{33}$$

Again, we derive the equations for the three-loop Matsubara correlations $q_{ab}(\tau,\tau')$ from the equations of motion [Eq. (27)], resulting in

$$0 = \frac{1}{2}q_{0,ab}^{-1}(\tau,\tau') - \frac{\hbar}{2}q_{ab}^{-1}(\tau,\tau') - \frac{J^2}{2\hbar}q_{ab}(\tau,\tau') + 6g\delta_{ab}\delta(\tau-\tau')q_{aa}(\tau,\tau) - \frac{48g^2}{\hbar}q_{ab}(\tau,\tau')^3 + \frac{12J^2g}{\hbar^2}q_{ab}(\tau,\tau')\sum_c\int d\tau'' q_{ac}(\tau,\tau'')^2. \tag{34}$$

Solutions of the self-consistency Eqs. (32) and (34) were attempted in a replica symmetric approximation and using Fourier transform techniques as described below. First, however let us turn to a description of the two nonperturbative approaches we have looked at, both also in a replica symmetric version.

VI. NONPERTURBATIVE THEORY

A. Replica symmetry

The nonperturbative theory is constructed in the RS approximation. We mention here that the effects of replica symmetry breaking on the low-temperature anomalies have been small for the semiclassical treatments.[8,9] The RS form of the Matsubara correlations is

$$q_{aa}(\tau,\tau') = q_d(\tau,\tau'), \tag{35a}$$

$$q_{ab}(\tau,\tau') = q \quad (\text{for } a \neq b), \tag{35b}$$

independent of the replicas a,b. The off-diagonal Matsubara correlation [Eq. (35b)] is assumed to be time independent. The argument is that the replicas are independent and time-translationally invariant, and that the origin of time could be chosen independently for each replica.[12]

The RS Ansatz allows us to decouple the replicas in the effective single-site action [Eq. (15)]. This concerns two terms. The first term to decouple is the nonlocal quartic interaction given in Eq. (16). We linearize this with a Gaussian variable $\bar{z}$. The second term to consider comes from the part of q_0^{-1} in Eq. (17) that involves $q_{ab}(\tau,\tau')$. This is decoupled by means of the Gaussian variable z. After decoupling, the effective single-site partition function [Eq. (13)] becomes

$$Z_{\text{eff}} = \int \mathcal{D}z\mathcal{D}\bar{z}\left\{\int \mathcal{D}u\,\exp\left(-\frac{1}{\hbar}\mathcal{S}_{\text{RS}}[u;z,\bar{z}]\right)\right\}^n, \tag{36}$$

where $\mathcal{D}z = dz/\sqrt{2\pi}\exp(-\frac{1}{2}z^2)$ and the same form for $\bar{z}$. The decoupled RS action reads

$$\mathcal{S}_{\text{RS}}[u;z,\bar{z}] = \int d\tau\left\{\frac{m}{2}\left[\frac{du(\tau)}{d\tau}\right]^2 - Jz\sqrt{q}u(\tau) + \frac{1}{2}[12gq_d(\tau,\tau) + J\bar{z}]u(\tau)^2 + gu(\tau)^4 - \frac{J^2}{2\hbar}\int d\tau'[q_d(\tau,\tau') - q]u(\tau)u(\tau')\right\}. \tag{37}$$

Substituting Eq. (36) in Eq. (18) gives for the free energy [Eq. (8)],

$$\beta f = -\int \mathcal{D}z\mathcal{D}\bar{z}\,\log\left\{\int \mathcal{D}u\,\exp\left(-\frac{1}{\hbar}\mathcal{S}_{\text{RS}}\right)\right\} + \frac{1}{\hbar}\mathcal{X}_{\text{RS}}[q], \tag{38}$$

where the nonfluctuating part is now defined as

$$\mathcal{X}_{\text{RS}}[q] = \frac{J^2}{4\hbar}\int d\tau d\tau'[q_d(\tau,\tau')^2 - q^2] - 3g\int d\tau q_d(\tau,\tau)^2. \tag{39}$$

Finally, the RS saddle-point Eq. (19) becomes

$$q_d(\tau,\tau') = \langle\langle u(\tau)u(\tau')\rangle\rangle_{z\bar{z}}, \tag{40a}$$

$$q = \langle\langle u(\tau)\rangle^2\rangle_{z\bar{z}}, \tag{40b}$$

where $\langle\cdots\rangle$ denotes an average mediated by the action $\mathcal{S}_{\text{RS}}$ and $\langle\cdots\rangle_{z,\bar{z}}$ the averages w.r.t. the Gaussians z and $\bar{z}$. The theory defined by Eqs. (37)–(39), (40a), and (40b) is nonlocal in Matsubara time. There are currently no analytic techniques available to solve the self-consistency problem for the Matsubara correlations in this theory nonperturbatively while keeping the full complexity arising from this fact. Two different methods will be used to deal with this problem, a numerical approach using quantum Monte Carlo simulations as proposed in Ref. 23 and the so-called static approximation due to Bray and Moore.[12]

B. Static approximation

In this approximation the nonlocal term [the third line in Eq. (37)] is approximated by taking for the diagonal Matsubara correlations a simple time-independent trial function,

$$q_d(\tau,\tau') = q_d, \tag{41}$$

which may but need not assumed to be equal to $q_d(\tau,\tau) \equiv q_d(0)$. Such static approximation scheme was introduced as a variational Ansatz in Ref. 12 when studying the spin-glass transition for the SK model generalized to quantum spins. After applying Eq. (41) we are able to linearize the nonlocal term of Eq. (37) by means of a further Gaussian transformation, defined by a Gaussian variable v. This results in the following static action:

$$\mathcal{S}_{\rm st}[u,v;z,\bar{z}] = \int d\tau \left\{ \frac{m}{2}\left[\frac{du(\tau)}{d\tau}\right]^2 + \frac{1}{2}v^2 - J\sqrt{C}vu(\tau) + d_1(z)u(\tau) + d_2(\bar{z})u(\tau)^2 + gu(\tau)^4 \right\} \quad (42)$$

with $C=\beta(q_d-q)$. The random parameters d_1 and d_2 are defined as

$$d_1(z) = -Jz\sqrt{q},$$

$$d_2(\bar{z}) = \frac{1}{2}[12gq_d(0) + J\bar{z}] \quad (43)$$

with $q_d(0)=q_d(\tau,\tau)$. The free energy [Eq. (38)] becomes

$$\beta f = -\int \mathcal{D}z\mathcal{D}\bar{z}\log\left\{\int \mathcal{D}u \int \frac{dv}{\sqrt{2\pi/\beta}}\exp\left(-\frac{1}{\hbar}\mathcal{S}_{\rm st}\right)\right\} + \frac{1}{\hbar}\mathcal{X}_{\rm RS}[q] \quad (44)$$

with the nonfluctuating part $\mathcal{X}_{\rm RS}[q]$ given by Eq. (39).

Before presenting the self-consistency relations for the order parameters, let us first take a closer look at the static action [Eq. (42)]. The parameters $d_1(z)$, $d_2(\bar{z})$, and g are the coupling constants of a potential energy for the system defined by the local *quantum* variable $u(\tau)$. The (quenched) Gaussians z and $\bar{z}$ imply that we have here a heterogeneous family of such systems. This results in a broad spectrum of *tunneling* and *vibrational excitations*, which we shall discuss in a separate section below.

Interestingly, there is another term in the action, namely, $-J\sqrt{C}vu(\tau)$, which is of a different nature. The constant $J\sqrt{C}$ defines a coupling constant for the bilinear interaction between the variable $u(\tau)$ and the *classical* (annealed) degree of freedom v. The latter is indeed a classical variable since it has no kinetic term associated with it. The appearance of this "annealed" degree of freedom is a result of formal mathematical analysis (as are the quenched variables z and $\bar{z}$). Both are "interpreted" and they acquire different meanings due to the different ways in which they appear in the theory. The z and $\bar{z}$ variables are *frozen*, resulting in an ensemble of double-well and single-well potentials whereas the variable v defines a *dynamical* degree of freedom. The coupling to v is entirely analogous to the coupling to a heat bath of phonons, as it is postulated in the phenomenological models of glassy low-temperature anomalies,[2–5] though the details are of course different. Whereas phenomenological models *postulate* a coupling of local degrees of freedom to the strain field of a heat bath of phonons as an additional ingredient, the coupling to a harmonic classical variable v in the present case *emerges* through the (approximate) mathematical treatment of quantum fluctuations. Incidentally the presence of a heat-bathlike background system could have been inferred directly from the appearance of retarded interactions in Eqs. (15)–(17) as such retarded interactions are the *usual* hallmark of effective descriptions of systems embedded into larger systems, after intergrating out the degrees of freedom of those larger systems.

Next we evaluate the free energy as a variational estimate w.r.t. the static Matsubara correlations $q_d(0)$, q_d, and q. The static formulation [Eqs. (42)–(44)] defines a theory local in time. We were able to find numerical solutions for the Matsubara correlations in two different approaches, a *three-variable* approach in terms of the variables $q_d(\tau,\tau)\equiv q_d(0)$, q_d, and q and a *two-variable* approach in terms of the variables q_d and q, assuming $q_d(0)=q_d$. The variational equations in the three-variable approach are

$$q_d(0) = \langle\langle u(\tau)^2\rangle\rangle_{z\bar{z}}, \quad (45a)$$

$$\frac{J}{\hbar}q_d\sqrt{C} = \langle\langle vu(\tau)\rangle\rangle_{z\bar{z}}, \quad (45b)$$

$$q = \langle\langle u(\tau)\rangle^2\rangle_{z\bar{z}}. \quad (45c)$$

Here $\langle\cdots\rangle$ denotes an average mediated by the static action [Eq. (42)] while $\langle\cdots\rangle_{z,\bar{z}}$ denotes the Gaussian averages over z and $\bar{z}$. In the two-variable approach the variational equations are

$$\left(\frac{J}{\hbar}\right)^2 C = -12\frac{g}{\hbar}(\langle\langle u(\tau)^2\rangle\rangle_{z\bar{z}} - q_d) + \frac{J}{\hbar\sqrt{q}}\langle z\langle u(\tau)\rangle\rangle_{z\bar{z}}, \quad (46a)$$

$$q = \langle\langle u(\tau)\rangle^2\rangle_{z\bar{z}}. \quad (46b)$$

We will solve the functional self-consistency Eqs. (45) and (46) reverting to an operator description, and using truncated Hilbert spaces as described in Sec. VII B 3 below.

Tunneling and vibrational excitations

The potential energy in the action [Eq. (42)] contains an ensemble of single-well and (asymmetric) double-well potentials because of the stochastic nature of the parameters $d_1(z)$ and $d_2(\bar{z})$ as defined in Eq. (43). These single-well and double-well potentials are responsible for, respectively, vibrational excitations and the characteristic tunneling excitations in the system.[9] We see that this potential structure arises naturally as a result of microscopic interactions defined by the model. In this context we mention the phenomenological soft-potential model[4,5] in which one *postulates* the existence of an ensemble of classical potentials $V(u)=d_1u+d_2u^2+gu^4$, providing a semiclassical analysis of its tunneling and vibrational states. Whereas that model assumes a *uniform* distribution of the parameters d_1 and d_2, the quantum statistical treatment of the microscopic model as presented here predicts a *Gaussian* distribution of the parameters $d_1(z)$ and $d_2(\bar{z})$. Furthermore, $d_1(z)$ and $d_2(\bar{z})$ are parameterized by the disorder strength J and the order parameters q and $q_d(0)$. The *collective* nature of the latter can be seen as the origin of universality of the low-temperature physics predicted by the model.

VII. NUMERICAL RESULTS

A. Scaling

For numerics and representation of results we represent the theory constructed in the previous sections in terms of

dimensionless variables and parameters. Starting from a microscopic length scale u_0 we define the following energy scales:

$$E_0 = \frac{\hbar^2}{mu_0^2}, \quad E_g = gu_0^4, \quad E_J = Ju_0^2, \tag{47}$$

where E_0 defines the quantum energy scale. The dimensionless ratios of the variables are

$$\tilde{u} = \frac{u}{u_0}, \quad \tilde{q} = \frac{q}{u_0^2}. \tag{48}$$

Those for the parameters are defined as

$$\tilde{g} = \frac{E_g}{E_0}, \quad \tilde{J} = \frac{E_J}{E_0}, \quad \tilde{T} = \frac{k_B T}{E_0} = \tilde{\beta}^{-1}. \tag{49}$$

Let us consider the relation between the dimensionless temperature $\tilde{T}$ and the absolute temperature T for the simple example of vitreous silica, the amorphous state of SiO_2. Taking a microscopic length scale $u_0 = 10^{-10}$ m and substituting the values of $\hbar, k_B$ and the mass m of SiO_2 in the definitions above, implies for this case that $\tilde{T}=1$ corresponds approximately to $T=1$ K. In this context we shall from here on look at the dimensionless temperature $\tilde{T}$ as an approximate representation of the absolute temperature.

In what follows we shall ignore writing the tildes on the dimensionless variables and parameters. One can show that the scaled form of all equations given in the previous sections is then obtained by setting $\hbar = m = 1$.

B. Matsubara correlations

1. Perturbative solutions at two-loop order

The perturbative Matsubara correlations were computed at two-loop order in the RS approximation. This requires solving the saddle-point Eq. (32) with $q_{aa}(\tau-\tau') = q_d(\tau-\tau')$ which is an $\hbar\beta$-periodic function and $q_{a\neq b}(\tau-\tau') = q$. We treated them in a Fourier-transformed representation. Our convention for the Fourier transform of $\hbar\beta$-periodic functions $f(\tau)$ is as follows:

$$f(\tau) = \sum_k e^{i\omega_k(\tau)} \hat{f}(\omega_k), \tag{50a}$$

$$\hat{f}(\omega_k) = \frac{1}{\hbar\beta} \int d\tau e^{-i\omega_k(\tau)} f(\tau) \tag{50b}$$

with Matsubara frequencies $\omega_k = \frac{2\pi}{\hbar\beta} k$ $(k = 0, \pm 1, \ldots)$. The advantage of this convention is that the dimension of the transformed quantity is equal to its original dimension. The Fourier transform of the saddle-point Eq. (32) requires computing the Fourier transform $\hat{q}_{ab}^{-1}(\omega_k)$ of the (functional) inverse kernel $q_{ab}^{-1}(\tau, \tau')$. Note that the latter defines an inverse w.r.t. both replica structure and Matsubara-time integration satisfying

$$\sum_c \int d\tau'' q_{ac}^{-1}(\tau - \tau'') q_{cb}(\tau'' - \tau') = \delta_{ab}\delta(\tau - \tau'). \tag{51}$$

Using Fourier transform relations requires that

$$\sum_c \hat{q}_{ac}^{-1}(\omega_k) \hat{q}_{cb}(-\omega_k) = \delta_{ab}/(\hbar\beta)^2 \tag{52}$$

for all k, i.e., up to a factor $1/(\hbar\beta)^2$ the Fourier transforms $\hat{q}_{ac}^{-1}(\omega_k)$ of the inverse kernel are equal to the corresponding elements of the matrix inverse $\hat{q}(\omega_k)_{ac}^{-1}$ of the $\hat{q}(\omega_k)$ matrix in replica space,

$$\hat{q}_{ab}^{-1}(\omega_k) = \hat{q}(\omega_k)_{ab}^{-1}/(\hbar\beta)^2. \tag{53}$$

The RS representation of the matrix elements $\hat{q}(\omega_k)_{ac}^{-1}$ in the $n \to 0$ limit are given by[18]

$$\hat{q}(\omega_k)_{aa}^{-1} = \frac{1}{\hat{q}_d(\omega_k) - \hat{q}(\omega_k)} - \frac{\hat{q}(\omega_k)}{[\hat{q}_d(\omega_k) - \hat{q}(\omega_k)]^2}, \tag{54a}$$

$$\hat{q}(\omega_k)_{a\neq b}^{-1} = -\frac{\hat{q}(\omega_k)}{[\hat{q}_d(\omega_k) - \hat{q}(\omega_k)]^2}, \tag{54b}$$

where $\hat{q}(\omega_k) = \hat{q}\delta_{k,0}$. Using Eqs. (53) and (54) in the Fourier transform of Eq. (32) leads to the following equations for the two-loop RS Matsubara correlations. First, for $k=0$ we have of Eq. (32),

$$\frac{1}{\hat{q}_d(\omega_0) - \hat{q}} - \frac{\hat{q}}{[\hat{q}_d(\omega_0) - \hat{q}]^2} = -2(\beta J)^2 \hat{q}_d(\omega_0) + 24g\beta \sum_k \hat{q}_d(\omega_k), \tag{55a}$$

$$-\frac{\hat{q}}{[\hat{q}_d(\omega_0) - \hat{q}]^2} = -2(\beta J)^2 \hat{q}, \tag{55b}$$

where Eq. (55a) represents the replica diagonal and Eq. (55b) the replica off-diagonal case. For $k \neq 0$ we only have to consider the replica-diagonal case, giving

$$\frac{1}{\hat{q}_d(\omega_k)} = \beta\omega_k^2 - 2(\beta J)^2 \hat{q}_d(\omega_k) + 24g\beta \sum_k \hat{q}_d(\omega_k). \tag{56}$$

In the high-temperature phase where $\hat{q}=0$ the $\hat{q}_d(\omega_k)$ are found numerically from Eqs. (55) and (56) by solving a single self-consistency equation for the variable $\hat{z}_1 = \Sigma_k \hat{q}_d(\omega_k) = q_d(0)$, namely,

$$\hat{z}_1 = \frac{1}{4\beta J^2} \sum_k (B_k - \sqrt{B_k^2 - 8J^2}) \tag{57}$$

in which $B_k = \omega_k^2 + 24g\hat{z}_1$. In the low-temperature phase where $\hat{q} \neq 0$, $\hat{z}_1$ can be determined analytically, entailing that the $\hat{q}_d(\omega_k)$ can be expressed in closed form as

$$\beta[\hat{q}_d(\omega_0) - \hat{q}] = \frac{1}{J\sqrt{2}}, \tag{58a}$$

$$\hat{q}_d(\omega_{k\neq 0}) = \frac{1}{4\beta J^2}(B_k - \sqrt{B_k^2 - 8J^2}), \tag{58b}$$

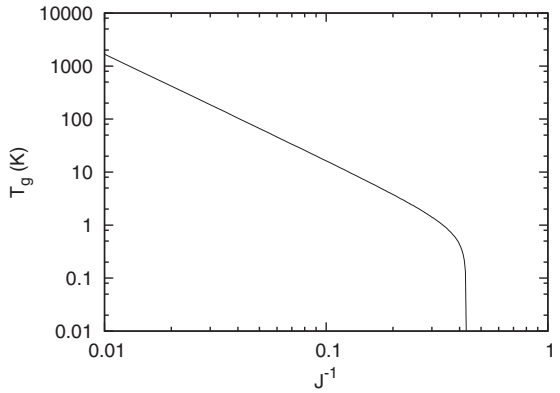

FIG. 2. Glass transition temperatures T_g vs J^{-1} at two-loop perturbation theory for $g=1$.

$$\hat{z}_1 = \frac{\sqrt{2}J}{12g}. \tag{58c}$$

The glass transition temperature T_g as a function of J (at $g=1$) is shown in Fig. 2. Glass transition temperatures for structural glasses are typically in the range between 500 and 1500 K. Clearly this requires J to be large. The majority of our results in the present study were therefore computed for a typical large J, $J=50$ giving $T_g \approx 500$ K.

Next is to discuss the solutions of Eq. (58) for the Matsubara correlations. The $q_d(\tau)$ were computed from a numerical inverse Fourier transformation of $\hat{q}_d(\omega_k)$. In Fig. 3 we plot the results for $q_d(\tau)-q$ and for a number of low temperatures. A selection of them is compared with the results of QMC simulations of the nonperturbative theory, which will be discussed in a section below. The solutions for the Matsubara correlation q are plotted in Fig. 4 in the low-temperature phase. From both Figs. 3 and 4 we conclude that the two-loop results are in reasonably good agreement with the QMC results.

The Fourier representation of the self-consistency equations for the Matsubara correlations in the low-temperature phase at three-loop order is given in the Appendix. The coupling between the Fourier modes at three-loop order contains a truly functional element via the function $\hat{z}_3(\omega_k)$. Although we succeeded in simplifying the problem to solve a set of only four coupled transcendental equations for the variables $\hat{z}_1$, $\hat{z}_2$, $\hat{q}_d(\omega_0)$, and q, we have so far been unable to solve them. In fact we suspect that physically acceptable solutions may not exist at three-loop order and an expansion to higher loop order might be necessary.

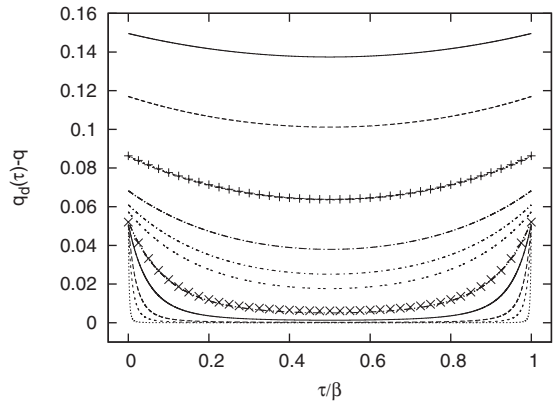

FIG. 3. Two-loop perturbative data for the function $q_d(\tau)-q$. Inverse temperatures (in K^{-1}) from top to bottom are $\beta=0.1,0.13,0.2,0.3,0.4,0.5,1,2,5,10,50$. Comparison with QMC solutions of the nonperturbative theory for $\beta=0.5$ and $\beta=1$ (marked by + and ×).

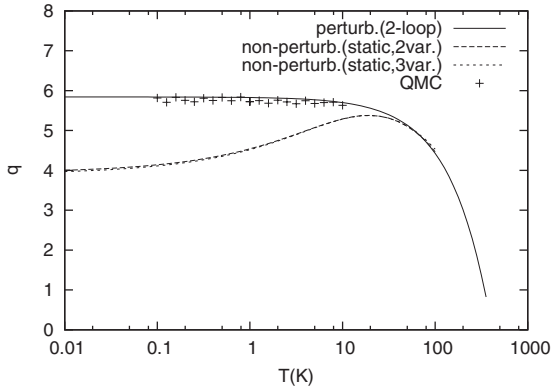

FIG. 4. Perturbative and nonperturbative data for the Matsubara correlation q in the low-temperature phase. Note the good agreement of two-loop perturbative data with nonperturbative data from quantum Monte Carlo simulations. Data of nonperturbative static approximations deviate from these in the low-temperature region.

2. Nonperturbative quantum Monte Carlo simulations

The Matsubara correlations $q_d(\tau)$ and q of the nonperturbative RS theory defined in Sec. VI A above, were evaluated with quantum Monte Carlo simulations. This involved solving the functional self-consistent relation (40). We used iterative QMC techniques along the lines of Ref. 23 starting with a set of initial values of $q_d(\tau)$ and q to be used as input for the action [Eq. (37)], after which they were updated in a path-integral Monte Carlo algorithm. This procedure was repeated ten times, resulting in reasonably good convergence of the Matsubara correlations. As regards to the algorithm, an update contained 10^5 Monte Carlo sweeps (taking data every tenth sweep), 5×10^4 equilibration sweeps, and 5×10^3 Gaussian $z,\bar{z}$ samples. The imaginary-time axis was discretized into 40 time slices. The results for $q_d(\tau)-q$ at a selected number of temperatures are plotted in Fig. 3. The results for the off-diagonal Matsubara correlation q are plotted separately in Fig. 4. As mentioned previously, they were found to be in good agreement with the solutions of the two-loop perturbative theory given in Eq. (58). The conclusion from the simulations is that they confirm the validity of the perturbative two-loop results for the Matsubara correlations.

3. Nonperturbative static solutions

The Matsubara correlations of the static approximation treated in Sec. VI B, were computed numerically. This involved solving the functional self-consistency relations (45) and (46). They were solved in the operator representation, for which the required Hamiltonian $\hat{H}_{\rm st}(\hat{p},\hat{u},v;z,\bar{z})$ is recon-

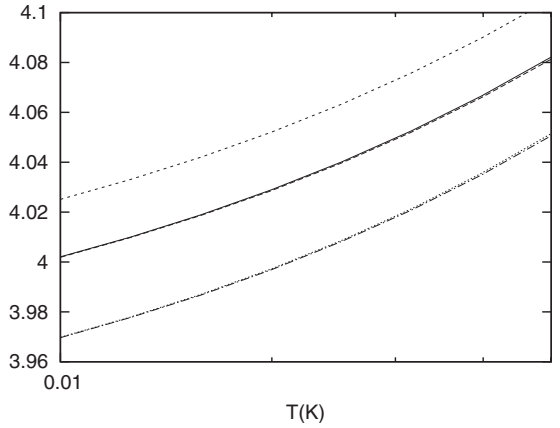

FIG. 5. The upper line shows $q_d(0)$ in the three-variable approach. The lowest pair of lines correspond to q_d and q in the three-variable approach whereas the pair of lines in the middle correspond to q_d and q in the two-variable approach.

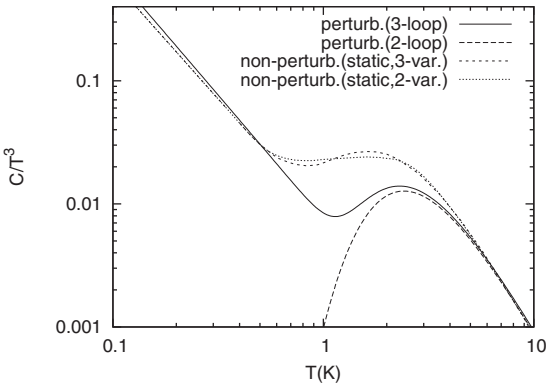

FIG. 6. Approximately linear specific heat $C \sim T^{1.02}$ ($T < 0.8$ K) and $C \sim T^{1.1}$ ($T < 0.5$ K) for, respectively, perturbative (three-loop) and nonperturbative (static) theories and a Bose peak at higher temperatures. The two-loop perturbative theory described only the vibrational excitations.

structed from the action [Eq. (42)]. Path integrals are then reexpressed in terms of traces over a suitable truncated Hilbert space. We used a bases of harmonic-oscillator eigenstates. The Gaussian integrals were computed with Gauss-Legendre quadratures.

The results for the replica off-diagonal Matsubara correlations q are plotted in Fig. 4 over a large temperature range. We believe the differences with the two-loop perturbative and QMC results seen here to be an artifact of the static approximation, which after all does not represent the true self-consistent solutions of the saddle-point Eq. (40).

Differences between the results of the two-variable and three-variable approaches are not visible on the scale used in Fig. 4. They are plotted separately in Fig. 5 for a selected range of low temperatures. The combination of order parameters $C = \beta(q_d - q)$, which can be seen as a susceptibilitylike variable, was found to be approximately equal for both, the two-variable and the three-variable approaches, with nearly constant numerical value $C \approx 17 \times 10^{-3}$ for $0 < T < 100$ K. Since this is very small, the values of q_d and q barely differ at low temperatures, as is indicated in Fig. 5. On the other hand, the two-variable and three-variable approaches do give rise to different values for the (q_d, q) pairs. Introduction of a third variable $q_d(0)$ in the three-variable approach leads to a depression of the values of q_d and q relative to those in the two-variable approach whereas $q_d(0)$ in the three-variable approach turns out to be larger than q_d and q within the two-variable solution.

C. Thermodynamics

1. Perturbative specific heat

To obtain an expression for the perturbative free energy we substitute Eqs. (14) and (28) in Eq. (30). We consider Fourier transforms as defined in Eq. (50) and the scaling introduced in Sec. VII A. The trace $\frac{1}{2}\mathrm{Tr}\,\hat{q}_0^{-1}\hat{q}$ diverges when substituting $\hat{q}_0^{-1}$ from its definition [Eq. (17)]. Instead we substitute the expression for $\hat{q}_0^{-1}$ determined by the saddle-point Eq. (32) and (34). The result is then finite up to an irrelevant infinite constant $\frac{1}{2}\mathrm{Tr}\,\hat{q}^{-1}\hat{q}$. The trace $\frac{1}{2}\mathrm{Tr}\log\hat{q}^{-1}$ can be shown to have the following RS representation:[18]

$$\frac{1}{2}\mathrm{Tr}\log\hat{q}^{-1} = -\frac{n}{2}\sum_k \left\{ \frac{\hat{q}(\omega_k)}{\hat{q}_d(\omega_k) - \hat{q}(\omega_k)} + \log[\hat{q}_d(\omega_k) - \hat{q}(\omega_k)] \right\}, \tag{59}$$

where n defines the number of replicas. Observe that when substituting $\hat{q}(\omega_k) = \hat{q}\,\delta_{k,0}$ the second part of Eq. (59) contains the divergent sum $-\frac{1}{2}\Sigma_{k\neq 0}\log\hat{q}_d(\omega_k)$. To deal with this we first substitute $\hat{q}_d(\omega_k)$ from Eq. (56) and (A5). From the result we isolate a divergent contribution of the following form $\frac{1}{2}\Sigma_k \log\{\beta(\omega_k^2 + 24g\hat{z}_1)\}$ with $\hat{z}_1 = \Sigma_k \hat{q}_d(\omega_k)$. This term, as part of Eq. (59) and Γ_{eff} in Eq. (28), should be exponentiated according to Eq. (21), defining the partition function of a simple harmonic oscillator with frequency $\omega_0 = \sqrt{24g\hat{z}_1}$. Consequently, we may replace $\frac{1}{2}\Sigma_k \log\{\beta(\omega_k^2 + \omega_0^2)\}$ by (β times) the free energy of a simple harmonic oscillator, giving $\log\sinh(\frac{1}{2}\beta\omega_0)$ which is now finite.

To compute the RS free energy numerically we have only the two-loop data from Eq. (58) at our disposal. The specific heat computed from the two-loop free energy did *not* result in a glassy low-temperature anomaly. Only vibrational excitations of the system featured here (see Fig. 6). On the other hand, when evaluating the free energy at three-loop order, a specific heat exhibiting the characteristic glassy low-temperature anomaly was obtained ($C \sim T^{1.02}$ for $T < 0.8$ K), though we had to use two-loop results for the Matsubara correlations in those expressions (as three-loop results are so far unavailable). The good agreement between two-loop Matsubara correlations and QMC results is thought to provide a reasonable justification for this approach.

2. Nonperturbative specific heat

The nonperturbative thermodynamics was evaluated in the static approximation. For this we used the free-energy expression (44) and the numerical results determined from Eqs. (45) and (46). This indeed reproduced the characteristic

glassy low-temperature specific-heat anomaly for both the two-variable and three-variable approaches (see Fig. 6). Again the low-temperature specific heat showed an approximately linear (in fact superlinear) temperature dependence $C \sim T^{1.1}$ for $T < 0.5$ K, in reasonable agreement also with experimental data.[1,24] These results should also be compared with and are indeed comparable to those of the translationally invariant model investigated in Ref. 9. We found little difference in the results for the two-variable and three-variable approaches at higher temperatures, as can be seen in Fig. 6. Differences between the three-loop perturbative specific heat and the nonperturbative "static" specific heat are restricted to the 0.5–5 K temperature region. This could be at least partly because of the strong temperature dependence of the static Matsubara correlations in this region, as displayed in Fig. 4 for the order parameter q.

Finally we remark that both the properties of the Bose peak at intermediate temperatures and the universal tunneling regime at low temperatures are governed by one and the same set of system parameters appearing in Eq. (42). No separate sets of assumptions were introduced to describe these two temperature regimes.

VIII. CONCLUSIONS

In summary, we have provided a fully quantum statistical analysis of a microscopic model of a glass, respecting global translation invariance. Until now such analysis was available only at a semiclassical level. We formulated an effective theory in terms of single-site path integrals and constructed perturbative and nonperturbative solutions of a set of self-consistency equations describing the system. Both resulted in an approximately linear specific heat at low temperatures, in good agreement with experiment.

The perturbation theory was formulated in terms of two-particle irreducible diagrams at two-loop and three-loop orders for the effective action. As solutions of the self-consistency equations at three-loop order remained unavailable, we resorted to investigate the reliability of our two-loop results using quantum Monte Carlo simulations. We found surprisingly good agreement of the Matsubara correlations obtained perturbatively and via QMC simulations.

Within a nonperturbative static approximation we obtain a description in terms of a glassy potential-energy landscape containing an ensemble of effective single-well and double-well potentials, much as in the soft-potential model[4,5] and in the semiclassical approach.[9] Interestingly there is an important difference, namely, the emergence of a coupling to an additional classical variable in a manner reminiscent of a coupling of local excitations to a heat bath as postulated within phenomenological models.[25]

It would be interesting to carry the perturbative approach to higher loop order or in fact attempt summations of infinite classes of 2PI diagrams. On another front, effects of replica symmetry breaking have not yet been looked at and are worth investigating (though in a semiclassical approach RSB effects were found to be weak[9]).

One of the motivations for the present investigation was to understand a phase transition observed in ultracold glasses more than a decade ago,[26] which has so far not found an explanation. Regrettably, the present study has not produced any progress in that particular direction. It might well be the case that an expansion of the present investigation in *both* directions mentioned above—including effects of replica symmetry breaking and inclusion of diagrams up to arbitrarily high loop order—would be required to reveal pertinent signatures of that phase transition.

APPENDIX

Here we present the Fourier-transformed RS representation of the three-loop perturbative Eq. (34) in the low-temperature phase. Considering the scaling introduced in Sec. VII A and using Eqs. (53) and (54), the Fourier transformation leads to the following set of equations. First, for $k=0$ we have

$$\frac{1}{\hat{q}_d(\omega_0)-\hat{q}} - \frac{\hat{q}}{[\hat{q}_d(\omega_0)-\hat{q}]^2} = -2(\beta J)^2\hat{q}_d(\omega_0) + 24g\beta\hat{z}_1 - 96(\beta g)^2\hat{z}_3(\omega_0) + 24(\beta J)^2 g\hat{q}_d(\omega_0)\beta(\hat{z}_2-\hat{q}^2), \tag{A1}$$

$$-\frac{\hat{q}}{[\hat{q}_d(\omega_0)-\hat{q}]^2} = -2(\beta J)^2\hat{q} - 96(\beta g)^2\hat{q}^3 + 24(\beta J)^2 g\hat{q}\beta(\hat{z}_2-\hat{q}^2), \tag{A2}$$

where Eq. (A1) represents the replica diagonal and Eq. (A2) the replica off-diagonal case. The last two terms in these equations define the three-loop extensions of the two-loop Eq. (55). Here we used the following definitions:

$$\hat{z}_2 = \sum_k \hat{q}_d(\omega_k)^2, \tag{A3}$$

$$\hat{z}_3(\omega_k) = \sum_{lm} \hat{q}_d(\omega_l)\hat{q}_d(\omega_m)\hat{q}_d(\omega_k-\omega_l-\omega_m). \tag{A4}$$

For $k \neq 0$ we only have to consider the replica-diagonal case, giving

$$\frac{1}{\hat{q}_d(\omega_k)} = \beta\omega_k^2 - 2(\beta J)^2\hat{q}_d(\omega_k) + 24g\beta\hat{z}_1 - 96(\beta g)^2\hat{z}_3(\omega_k) + 24(\beta J)^2 g\hat{q}_d(\omega_k)\beta(\hat{z}_2-\hat{q}^2), \tag{A5}$$

where the last two terms again represent the three-loop extensions of the two-loop equations. The solutions of Eq. (A1) and (A2) can no more be expressed in analytic form as was the case for the two-loop perturbative Eq. (58).

[1] R. C. Zeller and R. O. Pohl, Phys. Rev. B **4**, 2029 (1971).
[2] P. Anderson, B. Halperin, and S. Varma, Philos. Mag. **25**, 1 (1972).
[3] W. Phillips, J. Low Temp. Phys. **7**, 351 (1972).
[4] V. G. Karpov, M. I. Klinger, and F. Ignat'ev, Sov. Phys. JETP **57**, 439 (1983).
[5] U. Buchenau, Y. M. Galperin, V. L. Gurevich, D. A. Parshin, M. A. Ramos, and H. R. Schober, Phys. Rev. B **46**, 2798 (1992).
[6] C. C. Yu and A. J. Leggett, Comments Condens. Matter Phys. **14**, 23 (1988).
[7] A. L. Burin and Y. Kagan, Sov. Phys. JETP **82**, 159 (1996).
[8] R. Kühn and U. Horstmann, Phys. Rev. Lett. **78**, 4067 (1997).
[9] R. Kühn, Europhys. Lett. **62**, 313 (2003).
[10] V. L. Gurevich, D. A. Parshin, and H. R. Schober, Phys. Rev. B **67**, 094203 (2003).
[11] D. A. Parshin, H. R. Schober, and V. L. Gurevich, Phys. Rev. B **76**, 064206 (2007).
[12] A. Bray and M. Moore, J. Phys. C **13**, L655 (1980).
[13] T. M. Nieuwenhuizen and F. Ritort, Physica A **250**, 8 (1998).
[14] L. F. Cugliandolo, D. R. Grempel, and C. A. da Silva Santos, Phys. Rev. B **64**, 014403 (2001).
[15] D. Sherrington and S. Kirkpatrick, Phys. Rev. Lett. **35**, 1792 (1975).
[16] H. F. Trotter, Proc. Am. Math. Soc. **10**, 545 (1959).
[17] E. Nelson, J. Math. Phys. **5**, 332 (1964).
[18] M. Mezard, G. Parisi, and M. Virasoro, *Spin Glass Theory and Beyond* (World Scientific, Singapore, 1987).
[19] J. Cornwall, R. Jackiw, and E. Tomboulis, Phys. Rev. D **10**, 2428 (1974).
[20] H. Kleinert, Fortschr. Phys. **30**, 187 (1982).
[21] A. Crisanti and Umberto Marini Bettolo Marconi, Phys. Rev. E **51**, 4237 (1995).
[22] M. Thesen, Ph.D. thesis, Universität Heidelberg, 2003.
[23] D. R. Grempel and M. J. Rozenberg, Phys. Rev. Lett. **80**, 389 (1998).
[24] L. Gil, M. A. Ramos, A. Bringer, and U. Buchenau, Phys. Rev. Lett. **70**, 182 (1993).
[25] W. A. Phillips, *Amorphous Solids, Low-Temperature Properties* (Springer, Berlin, 1981).
[26] P. Strehlow, C. Enss, and S. Hunklinger, Phys. Rev. Lett. **80**, 5361 (1998).